# Exciton Coherence and Electron Energy Loss Spectroscopy of Conjugated Molecules

V. Chernyak, S. N. Volkov, and S. Mukamel
*Department of Chemistry, University of Rochester, P.O. RC Box 270216, Rochester, New York 14627-0216*
(Received 1 May 2000)

Signatures of the exciton coherence size, which controls the nonlinear optical response and luminescence of conjugated systems, in the electronic dynamic structure factor $S(\mathbf{q}, \omega)$ are calculated. We find that for small molecules the momentum dependence of the lowest exciton resonance is purely geometric, reflecting the molecular size rather than a universal exciton size, as suggested recently. For long chains the $\mathbf{q}$ dependence is determined by the interplay of the exciton size and the bond-alternation length scales.

DOI: 10.1103/PhysRevLett.86.995 PACS numbers: 34.80.Gs, 31.15.Ct, 82.80.Pv

The magnitude of the optical response of conjugated molecules and nanostructures and its scaling and saturation with molecule size depend primarily on the correlation among the optically generated electron-hole pairs which form excitons [1]. The exciton size has drawn considerable attention [2] since it directly controls the magnitude of optical nonlinearities, the radiative lifetime, and fluorescence [1,3]. It is further the key for understanding the transport and electroluminescence properties of conjugated polymers [1,3]. Determination of the exciton coherence size is thus of fundamental interest with important implications on the design of optical materials and devices [4–6]. Establishing relations between the exciton size and ground state properties, e.g., the bond- and length-alteration parameters, allows one to connect the optical properties of conjugated molecules to their chemical structure [7,8]. Exciton coherence also plays an important role in controlling the optical properties of donor/acceptor substituted molecules [8].

Electron energy loss spectroscopy (EELS) constitutes a powerful tool for the study of optically inaccessible high-wave-vector electronic excitations in the condensed phase. The basic quantity derived from EELS is the electronic dynamic structure factor $S(\mathbf{q}, \omega)$. When the incoming electron energy $E \sim 300$ keV is high compared to the $\Omega \sim 2$–$10$ eV energies of the tested transitions (which allows one to use the first Born approximation) and the effects of transverse photon exchange can be neglected since the energies $\Omega$ are nonrelativistic, the EELS signal is given by $I(\mathbf{q}, \omega) \sim q^{-4} S(\mathbf{q}, \omega)$, $\mathbf{q}$ being the momentum difference of the incident and scattered electrons, and $\omega$ is its energy loss. Theoretical analysis of recent experiments carried out on several conjugated molecules [9,10] focused on extracting the exciton coherence size in different materials. This was done by examining the momentum dependence of the frequency-integrated signal intensity of the lowest peak in the spectrum $I_0(\mathbf{q})$. Using a qualitative analogy with the static atomic structure factor, the characteristic size $q_0$ of $q^2 I_0(\mathbf{q})$ has been attributed to the size of the lowest exciton $l_e$: $q_0 \sim l_e^{-1}$. The experiments were then suggested to imply the existence of a $\sim 10$ Å universal exciton size in the molecules studied {e.g., sexithiophene, TPD [N,N′-diphenyl-N,N′-bis(3-methyl-phenyl)-1,1′-biphenyl-4,4′-diamine]} [10].

In this Letter we compute the structure factor of conjugated molecules using a Bloch representation of the reduced electronic density matrix and analyze the microscopic interpretation of EELS signals. Using elongated carotenoids with $N = 10$, 20, 40 double bonds (Fig. 1) as a representative example (for $\beta$-carotene $N = 9$ and it has additional methyl groups), we show that the previous interpretation is incorrect, since the momentum of the dynamic structure factor is related to the exciton center of mass rather than to the relative electron-hole motion.

The structure factor, defined as the correlation function of the charge density operator, may be expressed in terms of the density-density linear response function $\alpha(\omega; \mathbf{r}; \mathbf{r}')$ (see [11] for a precise definition of $\alpha$): $S(\mathbf{q}, \omega) = 2\,\mathrm{Im} \int d\mathbf{r}\, d\mathbf{r}'\, \alpha(\omega; \mathbf{r}; \mathbf{r}') \exp[i\mathbf{q} \cdot (\mathbf{r} - \mathbf{r}')]$. This allows one to compute $S(\mathbf{q}, \omega)$ using the same approaches developed for the optical response. Substituting the spectral decomposition of the linear response functions [8] into this equation, we obtain

$$S(\mathbf{q}, \omega) = \sum_{\nu} |\mathrm{Tr}[\mu(\mathbf{q}) \xi_{\nu}^{\dagger}]|^2 \frac{2\Gamma}{(\omega - \Omega_{\nu})^2 + \Gamma^2}. \quad (1)$$

Here $\Omega_{\nu}$ are the transition frequencies, $\Gamma$ is a dephasing rate, and $\mu_{mm'}(\mathbf{q})$ is the Fourier transform of the charge density operator, whose matrix elements are $\tilde{\mu}_{mm'}(\mathbf{r}) = \varphi_m(\mathbf{r})\varphi_{m'}(\mathbf{r})$, $\varphi_m(\mathbf{r})$ being single-electron atomic orbitals. $\xi_{\nu}$ are the transition density matrices with matrix elements

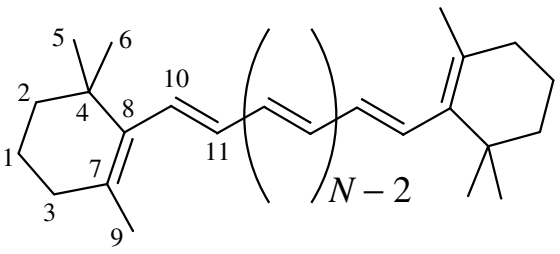


FIG. 1. Molecular structure and carbon atom numbering for a carotenoid with $N$ repeat units.

  

$\xi_{\nu,mm'}$, which act as operators in the single-electron space. In this Letter they are computed as the eigenmodes of the linearized time-dependent Hartree-Fock (TDHF) operator. However, other levels of theory (e.g., time-dependent density functional theory [11] and Green-function techniques [12]) may be used as well.

The transition density matrices (electronic normal modes) of a linear conjugated oligomer (Fig. 1) can be represented by matrix functions $\xi^{(\nu)}_{mm'}(j, j')$ where $j, j' = 1, \ldots, N$ denote the elementary (identical) repeat units whereas $j, j' = 0, N + 1$ describe the first and the last units, which may be different (e.g., donor/acceptor substituents). $m$ and $m'$ denote electronic orbitals within the elementary units. The electronic TDHF modes of an infinite oligomer can be recast in the Bloch representation. In a semi-infinite system with a left end ($j, j' = 0, 1, 2, \ldots$) a mode for $j, j' \gg l_e$ can be represented in the form

$$\xi^{(\nu)}_{mm'}(j, j') = \xi^{(\nu)}_{mm'}(j - j'; s)\exp(isj') + \xi^{(\nu)}_{mm'}(j - j'; -s)\exp[-isj' + iu^{(\nu)}_{\mathrm{L}}(s)]. \quad (2)$$

These modes are determined by the bands $\Omega^{(\nu)}(s)$ and the periodic parts of the Bloch functions given by $j$-dependent matrices $\xi^{(\nu)}_{mm'}(j; s)$. $s$ is the dimensionless momentum and $\nu$ parametrizes the various modes for a given momentum. $\exp[iu^{(\nu)}_{\mathrm{L}}(s)]$ is the exciton scattering amplitude on the left end of the molecule, $u^{(\nu)}_{\mathrm{L}}(s)$ being the phase shift. A similar representation for a mode is valid for a semi-infinite molecule with a right end ($j, j' = N + 1, N, N - 1, \ldots$) provided $N - j, N - j' \gg l_e$. Exciton scattering on the right end results in the phase shift $u^{(\nu)}_{\mathrm{R}}(s)$. The $s$-dependent phase shifts $u_{\mathrm{L}}(s)$ and $u_{\mathrm{R}}(s)$ can be obtained from a TDHF calculation in a semi-infinite system and are determined by the repeat unit which defines the band structure and by the end substituents. Both representations hold in the middle region of a finite molecule with $N \gg l_e$ provided $j, j', N - j, N - j' \gg l_e$. The required compatibility of the two representations provides the following quantization condition for the momenta in a finite oligomer:

$$u^{(\nu)}_{\mathrm{L}}(s_n) - u^{(\nu)}_{\mathrm{R}}(s_n) = 2s_n(N + 1) - 2\pi n, \quad (3)$$

$s_n$ being the solutions of Eq. (3) for $n = 0, \pm 1, \pm 2, \ldots$, and $\Omega^{(\nu)}_n = \Omega^{(\nu)}(s_n)$ are the transition frequencies. It immediately follows from Eq. (3) that at the band edge the quantization condition is defined by the derivatives $L_0 \equiv \frac{1}{2}[du^{(\nu)}(s)/ds]_{s=0}$ that describe the distance between one end of the molecule and the first node of a given mode. We found that for strong acceptors $L_0$ can reach the value of $L_0 \sim 5$; for unsubstituted oligomers $L_0 \approx -2$ and Eq. (3) yields $s_n = \pi n/(N + 3)$.

To obtain a simple expression for $I_0(\mathbf{q})$ for an intermediate size carotenoid, we assume that only carbon $\pi$ orbitals contribute to the structure factor and that we have two atoms in a unit cell, so that $m, m' = 1, 2$ in Eq. (2). Taking the lowest mode with $n = 1$, setting $s = 0$ in $\xi^{(\nu)}_{mm'}(j - j'; s)$, and neglecting the edge effects, i.e., assuming that Eq. (2) holds for all $j$ and $j'$, we obtain for the diagonal components $\xi_{mm}(j, j) \propto (-1)^m \sin[\pi(j + 1)/(N + 3)]$. Substitution into Eq. (1) yields

$$I_0(\mathbf{q}) \propto \frac{\sin^2\phi \sin^2(\mathbf{q}\cdot\mathbf{a}/2)\cos^2[(N + 3)\mathbf{q}\cdot\mathbf{b}/2]}{q^4 \sin^2[(\mathbf{q}\cdot\mathbf{b} - \phi)/2]\sin^2[(\mathbf{q}\cdot\mathbf{b} + \phi)/2]}. \quad (4)$$

Here $\phi = \pi/(N + 3)$, $\mathbf{b}$ is the lattice constant, and $\mathbf{a}$ is the vector connecting the two carbon atoms in a unit cell.

Equation (4) and the expression for $s_n$, which are asymptotically exact for large $N$, hold quite well even for small chains. This is shown by computations of $S(\mathbf{q}, \omega)$ [Eq. (1)] in elongated carotenoids with $N = 10$, 20, and 40 double bonds (Fig. 1). Starting with the INDO/S (intermediate neglect of differential overlap/spectroscopy) semiempirical Hamiltonian, the transition density matrices $\xi_\nu$ and frequencies $\Omega_\nu$ were obtained using the TDHF algorithm described earlier [8]. Figure 2 displays $S(\mathbf{q}, \omega)/q^2$ for $N = 10$ and 40, $\mathbf{q}$ is directed along the molecular axis, and $\Gamma \to 0$. The circles radii are proportional to $|\mathrm{Tr}[\mu(\mathbf{q})\xi^\dagger_\nu]|^2/q^2$, i.e., the form-factor oscillator strengths divided by the square of the momentum transfer, and the range of $q_z$ corresponds to the first Brillouin zone of an infinite polymer chain. The figure shows a clear band structure of electronic excitations for $N = 40$ with the lowest band edge at $\omega \approx 2.1$ eV. It is remarkable that this structure is still pronounced even for $N$ as low as 10. Figure 2 also shows the bottom of the second band at about 4 eV, which overlaps with the first band, and the third band just above 4.5–5 eV; both bands are more distinct for $N = 40$. At frequencies higher than 4 eV, exciton scattering at the end units therefore involves at least two bands, and it can be described by $n \times n$ scattering matrices instead of scattering phases, where $n$ is the number of bands involved.

For frequencies of 5 eV and higher, it becomes increasingly harder to identify the bands using Fig. 2. This, however, can be accomplished by examining 2D plots of the transition density matrices describing particular modes: the number of nodes in the off-diagonal (diagonal) direction gives the band number (the exciton number in the band); for example, the left panel in Fig. 3 shows the transition density matrix for the fifth electronic mode in the third band. Strongly hybridized modes resulting from mixing of modes of different bands do not show a clear node pattern. The mode shown in the right panel of Fig. 3 is a hybrid of the twentieth mode in the first band and the second mode in the fourth band.

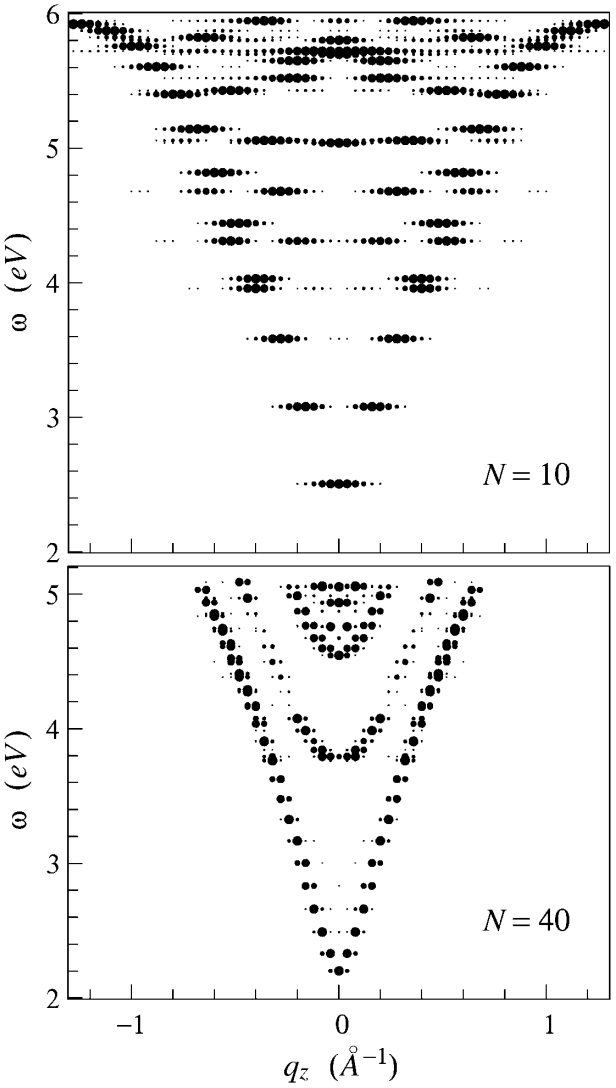


FIG. 2. Calculated normalized EELS signals $S(\mathbf{q},\omega)/q^2$, given as the circles radii, vs $q_z$ ($z$ is directed along the molecular axis) at values of $\omega$ corresponding to the frequencies of the 26 lowest electronic modes for a carotenoid with $N = 10$ repeat units (top panel) and the 50 lowest electronic modes for a carotenoid with $N = 40$ repeat units (bottom panel).

Figure 4 compares $q^2 I_0(\mathbf{q})$ computed for $N = 10$, 20, and 40 using Eq. (4) (dash-dotted lines) with the full INDO/S calculation (solid lines). The good agreement demonstrates the validity of the present Bloch representation for the EELS structure factor (band theory combined with exciton scattering on the ends) even for relatively short (e.g., $N = 10$) molecules. This means that when the lowest exciton peak is well resolved (which is the case for short chains), the $\mathbf{q}$ dependence of $q^2 I_0(\mathbf{q})$ solely reflects the physical size of the molecule, scales as $q_0 \propto N^{-1}$, and the exciton size $l_e$ affects only the absolute value of the signal. Our conclusions are at variance with Ref. [13] which argued that this scaling implies that the exciton size exceeds the molecular size.

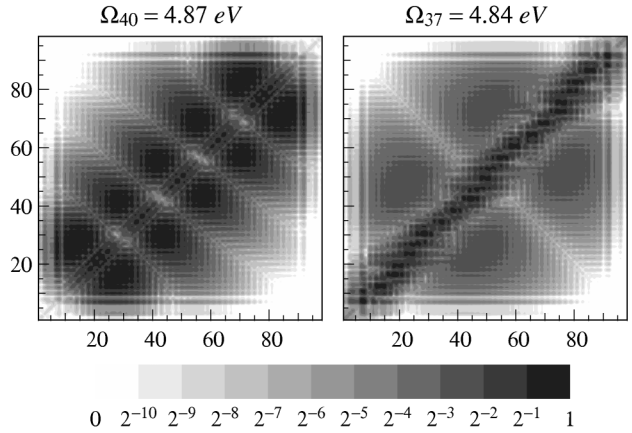


FIG. 3. Normalized modes $\xi^{(\nu)}_{mm'}$ of a carotenoid with $N = 40$ plotted for $\nu = 40$ and 37 on a logarithmic scale. The axes are labeled by the carbon atoms to which the $m$th or $m'$th atomic orbitals belong. Averaging is performed over all pairs of $m$th and $m'$th atomic orbitals corresponding to each particular pair of atoms [8]. The carbon atoms are numbered according to Fig. 1.

The structure factor $S(\mathbf{q},\omega)$ contains, however, more interesting dynamical information that can be obtained, e.g., by examining the momentum dependence of $I_j(\mathbf{q})$ for higher peaks ($j > 0$). Alternatively, one can study some

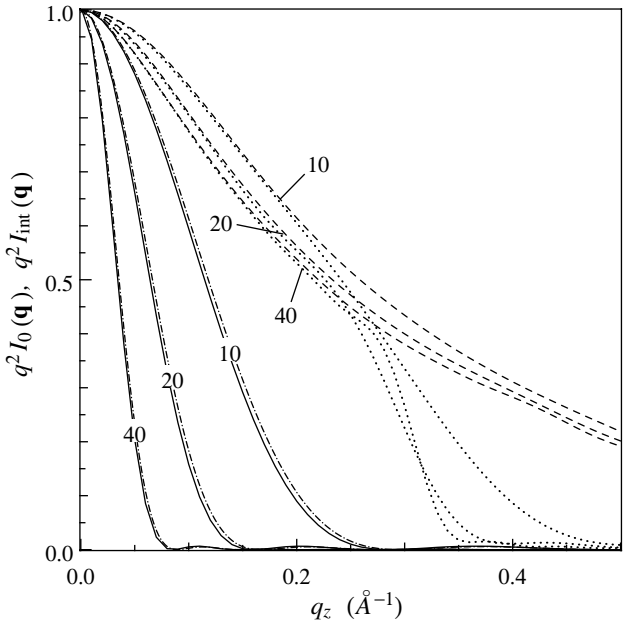


FIG. 4. Normalized integrated intensities of the lowest-frequency peak of the EELS signal $I_0(\mathbf{q})$, multiplied by $q^2$, vs $q_z$ (the high-resolution case): solid lines, INDO/S calculation, dash-dotted lines, the approximate expression Eq. (4). Normalized EELS signals integrated over frequencies from 0 to $\omega_{\max}$, $I_{\rm int}(\mathbf{q})$, multiplied by $q^2$, vs $q_z$ (the low-resolution case): dashed line, $\omega_{\max} = 5$ eV, dotted line, $\omega_{\max} = 3.7$ eV (includes only the modes of the first band). The three curves in each family correspond to carotenoids with $N = 10$, 20, and 40 repeat units, as indicated.

collective momentum-dependent quantities, such as the intensity $I_{\max}(\mathbf{q})$ of the dominant peak in the EELS spectrum or the frequency-integrated structure factor $I_{\text{int}}(\mathbf{q})$. The two coincide in the limit of long chains where several excitons overlap and form a narrow collective peak. In this case $I_{\max}(\mathbf{q})$ also coincides with $I_0(\mathbf{q})$, since the lowest peak becomes collective and represents the strongest rather than the lowest-frequency exciton. The analysis is particularly clear for an infinite polymer chain when the lowest peak in $S(\mathbf{q}, \omega)/q^2$ corresponds to the exciton with the momentum $s = \mathbf{q} \cdot \mathbf{b}$ in the lowest band and represents $I_0(\mathbf{q})$, as well as $I_{\max}(\mathbf{q})$ and $I_{\text{int}}(\mathbf{q})$. To explore how the exciton size $l_e$ affects $I_0(\mathbf{q})$, we assume that only the $\pi$ orbitals of the carbon atoms contribute and use a Pariser-Parr-Pople (PPP) type of Hamiltonian, with the nearest neighbor hopping constants $t_{\pm} = (1 \pm \zeta)t$, assuming weak Coulomb interaction case where $l_e \gg \zeta^{-1}$. The signal in this case is $\bar{I}_0(\mathbf{q}) \equiv q^2 I_0(\mathbf{q}) = (\zeta^2 + s^2)^{-1}|g(0; s)|^2$ [14], where $s = \mathbf{q} \cdot \mathbf{b}$. The first factor here shows the change of the structure factor on a typical momentum scale $s \sim \zeta$ related to the bond alternation. The second factor is the square of the eigenfunction $g(m; s)$ of the linearized TDHF equations representing a 1D particle on a lattice, taken for an exciton at $m = 0$, which depends parametrically on the center-of-mass momentum $s$. $|g(0; s)|^2$ changes on the scale $s \sim \zeta$ as well, which implies that $\bar{I}_0(\mathbf{q})$ is substantially nonzero at $\mathbf{q} \cdot \mathbf{b} \sim \zeta$ and we have $q_0 \sim \zeta/b$. However, the deviation of $\bar{I}_0(\mathbf{q})$ from a simple Lorentzian form carries information on the molecular-size dependence of the exciton size, since $l_e(s) \sim |g(0; s)|^{-2}$. For realistic PPP Hamiltonian parameters, $l_e(0) \sim \zeta^{-1}$, and $q_0 \sim \zeta^{-1}$.

Low-resolution calculations for carotenoids with $N = 10, 20, 40$ double bonds are displayed in Fig. 4. The dotted lines correspond to the frequency-integrated structure factor between $\omega = 0$ and 3.7 eV where only the first band contributes, and the dashed lines represent the integrated response between 0 and 5 eV where the second band may come into play as well. It is clear from the figure that the latter contribution can be safely neglected, since the dashed and dotted lines almost coincide for $q_z \leq 0.2$ Å where the largest contribution from the second band is to be expected. The dashed lines thus represent the first band only, or, equivalently, the lowest peak in the spectrum for the low-resolution case, i.e., $q^2 I_0(\mathbf{q})$. In contrast to the high-resolution case (solid and dash-dotted lines), the momentum scale $q_0$ for low resolution (dashed and dotted lines) is roughly the same for all three molecules.

In summary, when the molecule is sufficiently long so that the density of electronic states is high compared to the energy resolution, the lowest peak in $S(\mathbf{q}, \omega)$ corresponds to the lowest exciton with momentum $\mathbf{q}$ rather than to the lowest-frequency exciton. The characteristic momentum $q_0$ then reflects the combined effect of the bond-alternation parameter $\zeta$ and $l_e^{-1}$, and when $l_e \gg \zeta^{-1}$ we have $q_0 \sim \zeta$. However, even in this case $I_0(\mathbf{q})$ contains indirect information on the momentum dependence of the exciton size. In conjugated molecules typically $\zeta \sim l_e^{-1}$ [7], so that $q_0 \sim l_e^{-1}$, but this is a coincidence. A careful study of the momentum dependence of the integrated intensity of the higher peaks is required in order to extract meaningful information about excitons from EELS data in relatively short conjugated molecules.

The support of the National Science Foundation is gratefully acknowledged.

[1] M. Pope and C. E. Swenberg, *Electronic Processes in Organic Crystals and Polymers* (Oxford University Press, New York, 1999).
[2] *Optical Probes of Conjugated Polymers,* edited by Z. Valy Vardeny and L. Rothberg [Synth. Met. **116** (2001)].
[3] N. Kirova, S. Brazovskii, and A. R. Bishop, Synth. Met. **100**, 29 (1999).
[4] R. H. Friend *et al.,* Nature (London) **397**, 121 (1999).
[5] F. Hide, M. A. Diaz Garcia, B. J. Schwartz, and A. J. Heeger, Acc. Chem. Res. **30**, 430 (1997).
[6] D. G. Lidzey, D. D. C. Bradley, S. F. Alvarado, and P. F. Seidler, Nature (London) **386**, 135 (1997).
[7] S. Estemad and Z. G. Soos, in *Spectroscopy of Advanced Materials,* edited by R. J. H. Clark and R. E. Hester (Wiley, New York, 1991), p. 87.
[8] S. Tretiak, V. Chernyak, and S. Mukamel, J. Am. Chem. Soc. **119**, 11 408 (1997).
[9] E. Zojer *et al.,* Phys. Rev. B **56**, 10 138 (1997).
[10] M. Knupfer *et al.,* Phys. Rev. Lett. **83**, 1443 (1999); M. Knupfer *et al.,* Phys. Rev. B **61**, 1662 (2000).
[11] V. Chernyak and S. Mukamel, J. Chem. Phys. **112**, 3572 (2000).
[12] G. Strinati, Phys. Rev. B **29**, 5718 (1984); M. Rohlfing and S. G. Louie, Phys. Rev. Lett. **80**, 3320 (1998).
[13] M. Knupfer *et al.,* Chem. Phys. Lett. **318**, 585 (2000).
[14] V. Chernyak, S. N. Volkov, and S. Mukamel, J. Phys. Chem. B (to be published).